Available online at www.sciencedirect.com
SCIENCE DIRECT
Mathematical and Computer Modelling 42 (2005) 683–700
MATHEMATICAL AND COMPUTER MODELLING
www.elsevier.com/locate/mcm

Direct Simulation of the Uniformly Heated Granular Boltzmann Equation

I. M. GAMBA
Department of Mathematics
The University of Texas at Austin
Austin, TX 78712, U.S.A.
gamba@mail.ma.utexas.edu

S. RJASANOW
Fachrichtung 6.1 – Mathematik
Universität des Saarlandes
Postfach 151150 66041 Saarbrücken, Germany
rjasanow@num.uni-sb.de

W. WAGNER
Weierstrass Institute for Applied Analysis and Stochastics
Mohrenstr. 39, 10117 Berlin, Germany
wagner@wias-berlin.de

(Received and accepted February 2004)

Abstract—In this paper, we study properties of dilute granular flows, which are described by the spatially homogeneous uniformly heated inelastic Boltzmann equation. A new modification of the direct simulation Monte Carlo method is presented and validated using some analytically known functional of the solution. Then, the algorithm is applied to compute high velocity tails of the steady-state solution. The numerical results are used to check various theoretical predictions concerning the asymptotical behaviour of the tails. © 2005 Elsevier Ltd. All rights reserved.

Keywords—Granular matter, Boltzmann equation, Stochastic numerics.

1. INTRODUCTION

In recent years, a significant interest has been focused on the study of kinetic models for rapid granular flows [1,2]. Depending on the external conditions (geometry, gravity, interactions with surface of a vessel) granular systems may be in a variety of regimes, displaying typical features of solids, liquids, or gases and also producing novel statistical effects [3]. In the case of rapid, dilute flows, the binary collisions between particles may be considered the main mechanism of inter-particle interactions in the system. In such cases, methods of the kinetic theory of rarefied gases,

The first author has been supported by NSF under Grant DMS-0204568.
Support from the Institute for Computational and Engineering Sciences at The University of Texas at Austin is also gratefully acknowledged.

doi:10.1016/j.mcm.2004.02.047

based on the Boltzmann-Enskog equation have been applied [4–6]. Experimental and numerical data from molecular dynamics simulations (MD) [7–9] indicate that particle distribution functions are far from Maxwellian distributions when particles collide inelastically. Physically realistic regimes include excitation from the moving boundary, through-flow of air, fluidised beds, gravity, and other special conditions.

We take a simple model for a driving mechanism, called thermal bath, in which particles are assumed to be "uniformly heated" by uncorrelated random accelerations between the collisions. Such a model has been initially studied in [10] in the one-dimensional case, and in [11], in general dimension.

The first reference to non-Maxwellian steady-state solution was published in [11], by van Noije and Ernst, where by means of formal expansions in Sonine polynomials and *ad-hoc* closures, the authors conjectured the existence of steady-state solution with overpopulated "tails", i.e., slow decay rate of the distribution function for large velocities. Steady-state solutions were also studied by formal expansion methods for the Maxwell pseudomolecules model in [12–17]. These methods are based on small energy dissipation expansions and Fourier transforms. Existence, uniqueness, and regularity of the time dependent and steady-state solutions for the uniformly heated inelastic Boltzmann equation can be found in [18]. In addition, in [19], the authors proved rigorously the existence of radially symmetric steady-state solutions for the Maxwell pseudomolecules model. Rigorous mathematical properties of corresponding stationary solutions for the uniformly heated inelastic Boltzmann equation for the hard spheres model have been recently discussed in [20].

We consider the spatially homogeneous uniformly heated Boltzmann equation for granular media

$$\frac{\partial}{\partial t} f(t,v) - \beta \Delta_v f(t,v) = \gamma Q_\alpha(f)(t,v), \tag{1}$$

$$f(0,v) = f_0(v), \tag{2}$$

which describes the time evolution of the particle density

$$f : \mathbb{R}_+ \times \mathbb{R}^3 \to \mathbb{R}_+.$$

Here β and γ are some constants. The right-hand side of equation (1), known as the collision integral or the collision term, is most conveniently written in the weak form

$$\begin{aligned} &\int_{\mathbb{R}^3} Q_\alpha(f)(t,v)\varphi(v)\,dv \\ &= \frac{1}{2}\int_{\mathbb{R}^3}\int_{\mathbb{R}^3}\int_{S^2} B(|u|,\mu) f(t,v) f(t,w) \left(\varphi(v') + \varphi(w') - \varphi(v) - \varphi(w)\right) de\,dw\,dv, \end{aligned} \tag{3}$$

where $\varphi : \mathbb{R}^3 \to \mathbb{R}$ is a test function. Here $v, w \in \mathbb{R}^3$ are velocities, $u = v - w$ is the relative velocity and $v', w' \in \mathbb{R}^3$ are the postcollisional velocities defined by

$$\begin{aligned} v' &= \frac{1}{2}(v+w) + \frac{1-\alpha}{4}u + \frac{1+\alpha}{4}|u|e, \\ w' &= \frac{1}{2}(v+w) - \frac{1-\alpha}{4}u - \frac{1+\alpha}{4}|u|e, \end{aligned} \tag{4}$$

where $e \in S^2 \subset \mathbb{R}^3$ is a unit vector. Quantity μ is defined as

$$\mu = \frac{(u,e)}{|u|}. \tag{5}$$

Parameter $0 < \alpha \leq 1$ is called restitution coefficient. For $\alpha = 1$, the collisions are elastic and Q_1 coincides with the classical Boltzmann collision operator for a simple, dilute gas of particles [21].

Some special models for the (isotropic) kernel B are as follows.

1. The *hard spheres* model is described by the kernel

$$B(|u|, \mu) = C_1|u|, \qquad \text{for some } C_1 > 0. \tag{6}$$

2. The *Maxwell pseudomolecules* model is given by

$$B(|u|, \mu) = C_0, \qquad \text{for some } C_0 > 0. \tag{7}$$

   Here the collision kernel does not depend on the relative speed.

3. The *variable hard spheres* (VHS) model (cf. [22]) has an isotropic kernel

$$B(|u|, \mu) = C_\lambda |u|^\lambda, \qquad 0 \leq \lambda \leq 1, \tag{8}$$

   for some constants C_λ. This model includes, as particular cases, the hard spheres model (6) for $\lambda = 1$ and the case of the Maxwell pseudomolecules (7) for $\lambda = 0$.

The paper is organised as follows. In Section 2, we find an analytic solution of the temperature relaxation for the Maxwell pseudomolecules model (7). In Section 3, we recall some theoretical predictions concerning the asymptotic behaviour of the steady-state solution of equation (1). In Section 4, we describe a stochastic numerical algorithm for the uniformly heated inelastic Boltzmann equation. Compared to previous DSMC procedures it does not contain a time step error. In Section 5, we present the results of numerical tests. First, we use the analytically known time relaxation of the temperature to validate the numerical procedure. Then, high velocity tails of the steady-state solution are computed using the algorithm for different λ in (8). The results are compared with the available theoretical predictions.

2. TIME RELAXATION OF THE TEMPERATURE

All relevant physical quantities of the gas flow are computed as moments of the distribution function f or their combinations. Such moments are, for example, the density

$$\varrho(t) = \int_{\mathbb{R}^3} f(t, v)\, dv, \tag{9}$$

the momentum

$$m(t) = \int_{\mathbb{R}^3} v f(t, v)\, dv, \tag{10}$$

and the momentum flow

$$M(t) = \int_{\mathbb{R}^3} v v^T f(t, v)\, dv. \tag{11}$$

Using these moments, we define the bulk velocity

$$V(t) = \frac{m(t)}{\varrho(t)} \tag{12}$$

and the temperature

$$T(t) = \frac{1}{3\varrho(t)} \left(\sum_{i=1}^{3} M_{i,i}(t) - \varrho(t)|V(t)|^2 \right). \tag{13}$$

Note that in the spatially homogeneous case the following conservation properties hold, as an immediate consequence of (3). The density

$$\varrho(t) = \int_{\mathbb{R}^3} f(t,v)\,dv = \int_{\mathbb{R}^3} f_0(v)\,dv = \varrho_0 \tag{14}$$

and the momentum

$$m(t) = \int_{\mathbb{R}^3} vf(t,v)\,dv = \int_{\mathbb{R}^3} vf_0(v)\,dv = m_0$$

remain constant in time. Thus, according to (12), also the bulk velocity

$$V(t) = V_0 = \frac{m_0}{\varrho_0}$$

is a conserved quantity. Without loss of generality, we assume $\varrho_0 = 1$ and $V_0 = (0,0,0)^\top$ for the following discussion.

In contrast to the classical Boltzmann equation for elastic collisions, inelastic collisions ($0 < \alpha < 1$) dissipate energy. Thus, the temperature (cf. (13))

$$T(t) = \frac{1}{3}\int_{\mathbb{R}^3} |v|^2 f(t,v)\,dv$$

is a function of time. Taking $\varphi(v) = |v|^2$ in (3), we obtain (cf. [20])

$$|v'|^2 + |w'|^2 - |v|^2 - |w|^2 = -\frac{1-\alpha^2}{4}(1-\mu)|u|^2.$$

The second Green's formula leads to

$$\int_{\mathbb{R}^3} \Delta_v f(t,v)|v|^2\,dv = \int_{\mathbb{R}^3} f(t,v)\Delta_v|v|^2\,dv = 6\int_{\mathbb{R}^3} f(t,v)\,dv = 6\varrho_0 = 6.$$

Thus, the time evolution of the temperature is determined by relation (cf. (3))

$$\frac{dT}{dt} = 2\beta - \gamma\frac{1-\alpha^2}{24}\int_{\mathbb{R}^3}\int_{\mathbb{R}^3} B_1(|u|)|u|^2 f(v)f(w)\,dw\,dv, \tag{15}$$

where

$$B_1(|u|) = \int_{S^2} (1-\mu)B(|u|,\mu)\,de.$$

In the special case of Maxwell pseudomolecules (7), we obtain

$$B_1(|u|) = 4\pi C_0$$

so that (15) takes the form

$$\frac{dT}{dt} = 2\beta - \gamma\pi C_0\left(1-\alpha^2\right)T.$$

Thus, the time relaxation of the temperature is

$$T(t) = T_0 e^{-\gamma\pi C_0(1-\alpha^2)t} + T_\infty\left[1 - e^{-\gamma\pi C_0(1-\alpha^2)t}\right], \tag{16}$$

where

$$T_0 = \frac{1}{3}\int_{\mathbb{R}^3} |v|^2 f_0(v)\,dv, \qquad T_\infty = \frac{2\beta}{\gamma\pi C_0(1-\alpha^2)}. \tag{17}$$

3. ASYMPTOTIC PROPERTIES OF THE STEADY-STATE SOLUTION

Asymptotic properties of stationary solutions for the uniformly heated inelastic Boltzmann equation (1) have been recently discussed in many publications [11,12,19,20,23]. One of the most interesting related questions is the asymptotic behaviour of the steady-state distribution function

$$f_\infty(v) = \lim_{t\to\infty} f(t,v) \tag{18}$$

for large $|v|$ (high energy tails). It is worth to note that there is no such solution for the uniformly heated elastic Boltzmann equation, since the kinetic energy will increase linearly in time.

It has been recently shown in [12,16,20] that a typical tail for the inelastic variable hard spheres model (8) is expected to be given by the formula

$$f_\infty(v) \sim \exp\left(-a|v|^b\right), \qquad |v| \to \infty, \tag{19}$$

where a depends on the quotient of the energy dissipation rate and the heat bath temperature and b depends on the balance between the diffuse forcing term and the loss term of the collisional integral in the Boltzmann equation (1).

For instance, for the inelastic hard spheres (6), the exponent, or tail order is $b = 3/2$. This fact was noticed first in [11] by searching for the radially symmetric steady-state solution of a pointwise partial differential equation which was obtained using high velocities estimates to the loss term of the collision integral neglecting the gain term. Some arguments which justify this fact at a physical level of rigour and using an *a priori* assumption (19) were presented in a recent paper by Ernst and van Noije [11]. However, a rigorous pointwise lower estimate was obtained in [20] by means of strong comparison principle arguments, borrowing classical nonlinear PDE techniques to obtain pointwise bounds for regular solutions. Indeed, for the inelastic hard spheres model, the authors have proved in [20] the existence, uniqueness, and regularity of the time dependent and steady-state solutions for the uniformly heated inelastic Boltzmann equation (1). In particular, they showed the existence of the steady-state solution for the hard spheres model in the Schwartz space of rapidly decaying smooth functions, with a lower pointwise bound

$$f(v) \geq A \exp\left(-a|v|^{3/2}\right), \qquad |v| \geq R.$$

We emphasise that the appearance of the "3/2" exponent is a specific feature of the uniformly heated inelastic Boltzmann equation for the hard spheres model which can also be predicted by dimensional arguments (cf. [11]).

While the Maxwell pseudomolecules model (7) is good for an approximate description of integral quantities (see, for example, [24] for a comparison of the Maxwell pseudomolecules and hard spheres models in a shear flow problem), it leads to different behaviour of the tails compared to the hard spheres model. This can be observed when looking for approximate high-energy solutions of the inelastic Boltzmann-Fokker-Planck model when neglecting the gain part of the collision integral. The uniformly heated inelastic Boltzmann equation for the Maxwell pseudomolecules model results in a high-velocity tail with asymptotic behaviour (see [18])

$$f_\infty(v) \sim \exp(-a|v|), \qquad |v| \to \infty. \tag{20}$$

As a general rule, the exponents in the tails are expected to depend on the driving and collision mechanisms [16,25,26]. In fact, deviations of the steady states of granular systems from Maxwellian equilibria ("thickening of tails") is one of the characteristic features of dynamics of granular systems, and has been an object of intensive study in the recent years [8,27–29]. However, when different exponent $\lambda \neq 0, 1$ in the VHS model (8) is considered as usually done

for classical (elastic) Boltzmann equation, there is no rigorous proof of existence of steady-state solutions.

We expect that a technical and tedious extension of the analytical methods developed in [20] for existence, regularity, and pointwise lower estimates, and in [26] for the L^1-weighted tail control, indicates that the uniformly heated inelastic Boltzmann equation for the VHS model (8) results in a high-velocity tail with asymptotic behaviour

$$f_\infty(v) \sim \exp\left(-a|v|^{1+\lambda/2}\right), \qquad |v| \to \infty. \tag{21}$$

Our numerical results presented in Section 5 support this conjecture.

4. A DIRECT STOCHASTIC SIMULATION ALGORITHM

The main idea of all particle methods for the Boltzmann equation (1) is an approximation of the time dependent family of measures

$$f(t,v)\,dv, \qquad t > 0,$$

by a family of point measures

$$\nu(t,dv) = \frac{1}{n}\sum_{j=1}^{n} \delta_{v_j(t)}(dv)$$

defined by the system of particles

$$(v_1(t), \ldots, v_n(t)). \tag{22}$$

Thus, the weights of the particles are $1/n$ and $v_j(t) \in \mathbb{R}^3$ denote their velocities. The behaviour of system (22) can be briefly described as follows. The first step is an approximation of the initial measure (cf. (2))

$$f_0(v)\,dv$$

by a system of particles (22) for $t = 0$. Then, particles are continuously subjected to a Gaussian white noise forcing and obtain the kinetic energy executing individual Brownian motion between the collisions. The velocity of a single particle after a time s of Brownian motion is given by

$$v_j(t+s) = v_j(t) + \sqrt{2\beta s}\xi, \tag{23}$$

where $\xi \in \mathbb{R}^3$ is a random variable distributed according to the normalised Gaussian. The inelastic collisions take place in randomly distributed discrete time points dissipating the kinetic energy of the particles. The collision simulation is the most crucial part of the whole procedure. The behaviour of the collision process is as follows. The waiting time τ between the collisions can be defined either as a random variable with the distribution

$$\mathrm{Prob}\{\tau \geq t\} = \exp\left(-\hat{\pi}t\right),$$

where

$$\hat{\pi} = \frac{1}{2n}\sum_{1\leq i\neq j\leq n} B_{\max}(i,j)$$

and

$$\int_{S^2} B(|v_i - v_j|, \mu)\,de \leq B_{\max}(i,j), \tag{24}$$

or as a deterministic object by

$$\tau = \hat{\pi}^{-1}.$$

Majorant (24) can be obtained for the VHS-model (8) using an *a priori* known bound $U_{\max}$ for the maximal relative speed of particles

$$\gamma \int_{S^2} B(|v_i - v_j|, \mu)\, de = 4\pi\gamma C_\lambda |v_i(t) - v_j(t)|^\lambda \le 4\pi\gamma C_\lambda \left(U_{\max}\right)^\lambda .$$

Thus, we get a constant majorant

$$B_{\max}(i,j) = B_{\max} = 4\pi\gamma C_\lambda \left(U_{\max}\right)^\lambda \tag{25}$$

and

$$\hat{\pi} = 2\pi\gamma C_\lambda (n-1) \left(U_{\max}\right)^\lambda .$$

Then, the collision partners (i.e., the indices i and j) must be chosen. Since majorant $B_{\max}$ in (25) is a constant, the parameter i is to be chosen according to the probability $1/n$, i.e., uniformly from the set $\{1, \ldots, n\}$. Given i, parameter j is chosen according to the probability $1/(n-1)$, i.e., uniformly from the set $\{1, \ldots, n\} \setminus \{i\}$.

Given i and j, the collision is fictitious with probability

$$1 - \left(\frac{|v_i - v_j|}{U_{\max}}\right)^\lambda , \tag{26}$$

otherwise, vector e is uniformly distributed on the surface of the unit sphere S^2 and the postcollisional velocities v_i' and v_j' can be computed corresponding to the collision transformation (4). Note that velocities v_i and v_j of the collision partners have to be updated corresponding to (23) before computing the probability of fictitious collision according to (26).

The majorant $U_{\max}$ for the maximal relative velocity of the particle system can be obtained using the numerical bulk velocity

$$V = \frac{1}{n} \sum_{j=1}^{n} v_j \tag{27}$$

as follows

$$\max_{i,j} |v_i - v_j| \le \max_{i,j} \left(|v_i - V| + |V - v_j|\right) = 2 \max_i |v_i - V| = U_{\max}.$$

Before giving a formal description of our algorithm, we discuss some results known from the literature. The direct simulation Monte Carlo method (DSMC) introduced by Bird [30] is the most popular method for the numerical simulation of rarefied gases in many applications. The application of the DSMC to inelastic Boltzmann equation without any additional force (i.e., $\beta = 0$ in (1)) is straightforward and was described by Brey *et al.* [31] in 1996. Only one modification is needed, the postcollisional velocities have to be computed in accordance with (4).

However, the introduction of some additional force changes the situation. In [32], Montanero and Santos describe a variant of the DSMC procedure for three different forces injecting additional energy to the particle system. The case of the stochastic thermostat is equivalent to the uniformly heated inelastic Boltzmann equation (1) for $\beta > 0$. In order to be able to take into account both, continuous white noise forcing and discrete collisions, the authors separate these processes using some time step parameter Δt. In the collision stage, the particles collide without being accelerated by white noise forcing. The number of collisions is defined by the collision frequency. Then, the velocities of all particles are adapted according to (23). In our specific situation, we avoid the splitting error, which, by the way, is also not present in standard DSMC for the spatially homogeneous elastic Boltzmann equation. It will have to be decided by further investigations,

if this modification (joint modelling of acceleration and collisions) is of any significance in the spatially inhomogeneous case.

In [33], Barrat *et al.* present an extended study of a one-dimensional gas of inelastic particles using, among other methods, DSMC. The authors consider both heated and unheated inelastic particles and present a series of numerical results for the steady-state solution and its tails. However, the one-dimensional Boltzmann equation is only a rough model for physical three-dimensional case and the particular DSMC procedure used is not described in the paper.

In the present paper, we describe a modification of the DSMC method for the uniformly heated inelastic Boltzmann equation which does not involve any time-step error. This is achieved by not separating white noise forcing and discrete collisions. In order to increase the efficiency of the algorithm, we do not update all particle velocities at any time. Instead, we update the velocities only if a pair of particles is chosen for a binary collision or if the state of the whole system is required (computation of the moments). The prize for this simplification is that we need to know the time at which the particle was updated last time. Thus, additional storage is needed and the form of particles will be (v_j, t_j), where $v_j \in \mathbb{R}^3$ is the velocity and $t_j \in \mathbb{R}_+$ is the time of its last update.

Now we formulate the stochastic algorithm for the numerical solution of equation (1) on the time interval $[0, t_{\max}]$.

ALGORITHM.

1. initial distribution
   1.1 set time to zero $t = 0$;
   1.2 for $j = 1, \ldots, n$ generate the particles (v_j, t_j) with
      1.2.1 v_j distributed according to $f_0(v)$,
      1.2.2 $t_j = 0$;
   1.3 compute the bulk velocity V corresponding to

$$V = \frac{1}{n} \sum_{j=1}^{n} v_j;$$

   1.4 compute the majorant $U_{\max}$ corresponding to

$$U_{\max} = 2 \max_i |v_i - V|$$

2. repeat until $t \geq t_{\max}$
   2.1 compute the time counter τ

$$\tau = \frac{1}{2\pi\gamma C_\lambda (n-1) (U_{\max})^\lambda} \ln(-r_1);$$

   2.2 update the time of the system

$$t := t + \tau;$$

   2.3 define the index i

$$i = [r_2 \cdot n] + 1;$$

   2.4 define the index j repeating

$$j = [r_3 \cdot n] + 1$$

   until $j \neq i$;

2.5 update the velocities v_i and v_j corresponding to (23)

$$v_i := v_i + \sqrt{2\beta(t - t_i)}\xi_1, \qquad v_j := v_j + \sqrt{2\beta(t - t_j)}\xi_2;$$

2.6 update the times of the particles i and j

$$t_i = t, \qquad t_j = t;$$

2.7 update the majorant $U_{\max}$

$$U_{\max} = \max\{U_{\max}, |v_i - V|, |v_j - V|\};$$

2.8 decide whether the collision is fictitious. If

$$r_4 \leq 1 - \left(\frac{|v_i - v_j|}{U_{\max}}\right)^{\lambda}$$

then continue with Step 2.1, else

2.9 compute the postcollisional velocities

$$v_i := \frac{1}{2}(v_i + v_j) + \frac{1-\alpha}{4}(v_i - v_j) + \frac{1+\alpha}{4}|v_i - v_j|e,$$
$$v_j := \frac{1}{2}(v_i + v_j) - \frac{1-\alpha}{4}(v_i - v_j) - \frac{1+\alpha}{4}|v_i - v_j|e.$$

2.10 update the majorant $U_{\max}$

$$U_{\max} = \max\{U_{\max}, |v_i - V|, |v_j - V|\}$$

and continue with Step 2.1.

3. final step

3.1 update the velocities of all particles

$$v_i := v_i + \sqrt{2\beta(t_{\max} - t_i)}\xi_i, \qquad i = 1, \ldots, n;$$

3.2 compute the numerical moments of the distribution

$$m_\varphi(t_{\max}) = \frac{1}{n}\sum_{j=1}^{n}\varphi(v_j), \qquad \varphi(v) = 1, v, vv^T, v|v|^2.$$

In the above algorithm, the random numbers r_1, r_2, r_3, and r_4 are uniformly distributed on the interval $(0, 1)$ while the three-dimensional vectors ξ_i are distributed according to the normalised Gaussian. Vector e used in Step 2.9 is uniformly distributed on the unit sphere.

REMARK 1. The above algorithm is not completely conservative, i.e., the bulk velocity will change during the time. However, our numerical tests show only very small deviation of the bulk velocity from its initial value defined in (27).

REMARK 2. If the moments of the distribution function are to be computed in some discrete points $t_m = m\Delta t$, $m = 1, \ldots, M$, $\Delta t = t_{\max}/M$, then it is necessary to stop the process at time $t \geq t_m$, to update all velocities as in Step 3.1 of the algorithm and then to compute (Step 3.2) and to store the moments for further use.

5. NUMERICAL EXAMPLES AND TESTS

5.1. Statistical Notions

First, we introduce some definitions and notations that are helpful for the understanding of stochastic numerical procedures. Functionals of form (cf. (9)–(11))

$$F(t) = \int_{\mathbb{R}^3} \varphi(v) f(t,v)\, dv \tag{28}$$

are approximated by the random variable

$$\xi^{(n)}(t) = \frac{1}{n} \sum_{i=1}^{n} \varphi(v_i(t)), \tag{29}$$

where $(v_1(t), \ldots, v_n(t))$ are the velocities of the particle system. In order to estimate and to reduce the random fluctuations of estimator (29), a number N of independent ensembles of particles is generated. The corresponding values of the random variable are denoted by

$$\xi_1^{(n)}(t), \ldots, \xi_N^{(n)}(t).$$

The *empirical mean value* of the random variable (29)

$$\eta_1^{(n,N)}(t) = \frac{1}{N} \sum_{j=1}^{N} \xi_j^{(n)}(t) \tag{30}$$

is then used as an approximation to functional (28). The error of this approximation is

$$e^{(n,N)}(t) = \left| \eta_1^{(n,N)}(t) - F(t) \right|$$

and consists of the following two components.

The *systematic error* is the difference between the mathematical expectation of the random variable (29) and the exact value of the functional, i.e.,

$$e_{\text{sys}}^{(n)}(t) = E\xi^{(n)}(t) - F(t).$$

The *statistical error* is the difference between the empirical mean value and the expected value of the random variable, i.e.,

$$e_{\text{stat}}^{(n,N)}(t) = \eta_1^{(n,N)}(t) - E\xi^{(n)}(t).$$

A *confidence interval* for the expectation of the random variable $\xi^{(n)}(t)$ is obtained as

$$I_p = \left[\eta_1^{(n,N)}(t) - \lambda_p \sqrt{\frac{\operatorname{Var} \xi^{(n)}(t)}{N}}, \eta_1^{(n,N)}(t) + \lambda_p \sqrt{\frac{\operatorname{Var} \xi^{(n)}(t)}{N}} \right], \tag{31}$$

where

$$\operatorname{Var} \xi^{(n)}(t) := E\left[\xi^{(n)}(t) - E\xi^{(n)}(t) \right]^2 = E\left[\xi^{(n)}(t) \right]^2 - \left[E\xi^{(n)}(t) \right]^2 \tag{32}$$

is the *variance* of the random variable (29), and $p \in (0,1)$ is the *confidence level*. This means that

$$\text{Prob}\left\{E\xi^{(n)}(t) \notin I_p\right\} = \text{Prob}\left\{\left|e_{\text{stat}}^{(n,N)}(t)\right| \geq \lambda_p \sqrt{\frac{\text{Var}\,\xi^{(n)}(t)}{N}}\right\} \sim 1 - p.$$

Thus, the value

$$c^{(n,N)}(t) = \lambda_p \sqrt{\frac{\text{Var}\,\xi^{(n)}(t)}{N}}$$

is a probabilistic upper bound for the statistical error.

In the calculations, we use a confidence level of $p = 0.999$ and $\lambda_p = 3.2$. The variance is approximated by the corresponding empirical value (cf. (32)), i.e.,

$$\text{Var}\,\xi^{(n)}(t) \sim \eta_2^{(n,N)}(t) - \left[\eta_1^{(n,N)}(t)\right]^2,$$

where

$$\eta_2^{(n,N)}(t) = \frac{1}{N}\sum_{j=1}^{N}\left[\xi_j^{(n)}(t)\right]^2$$

is the *empirical second moment* of the random variable (29).

5.2. Relaxation of the Temperature

In this section, we validate the stochastic algorithm formulated in Section 4, using the analytically known relaxation of the temperature (cf. (16),(17)) in case of Maxwell pseudomolecules.

EXAMPLE 3. We use the Maxwell distribution

$$f_0(v) = \frac{1}{(2\pi)^{3/2}} e^{-|v|^2/2} \tag{33}$$

as the initial condition and the following set of parameters in (1),(4),(7)

$$\beta = 1, \qquad \gamma = 4, \qquad \alpha = \frac{1}{2}, \qquad C_0 = \frac{1}{4\pi}.$$

Thus, we obtain (cf. (17))

$$T_0 = 1, \qquad T_\infty = \frac{8}{3}$$

and (cf. (16))

$$T(t) = e^{-(3/4)t} + \frac{8}{3}\left(1 - e^{-(3/4)t}\right). \tag{34}$$

Here, the temperature increases monotonically in time.

The numerical results for Example 3 are displayed in Figure 1, where the dashed lines represent the analytical solution (34) on the time interval $[2.0, 8.0]$ while the pairs of solid lines represent the confidence intervals (31) obtained using $N = 10000$ independent ensembles.

It is almost impossible to see any difference between the numerical and the analytical solution in a figure for $n = 16384$, so we present the corresponding results in Table 1.

The second column of Table 1 shows the maximal error of the temperature on the whole time interval computed as

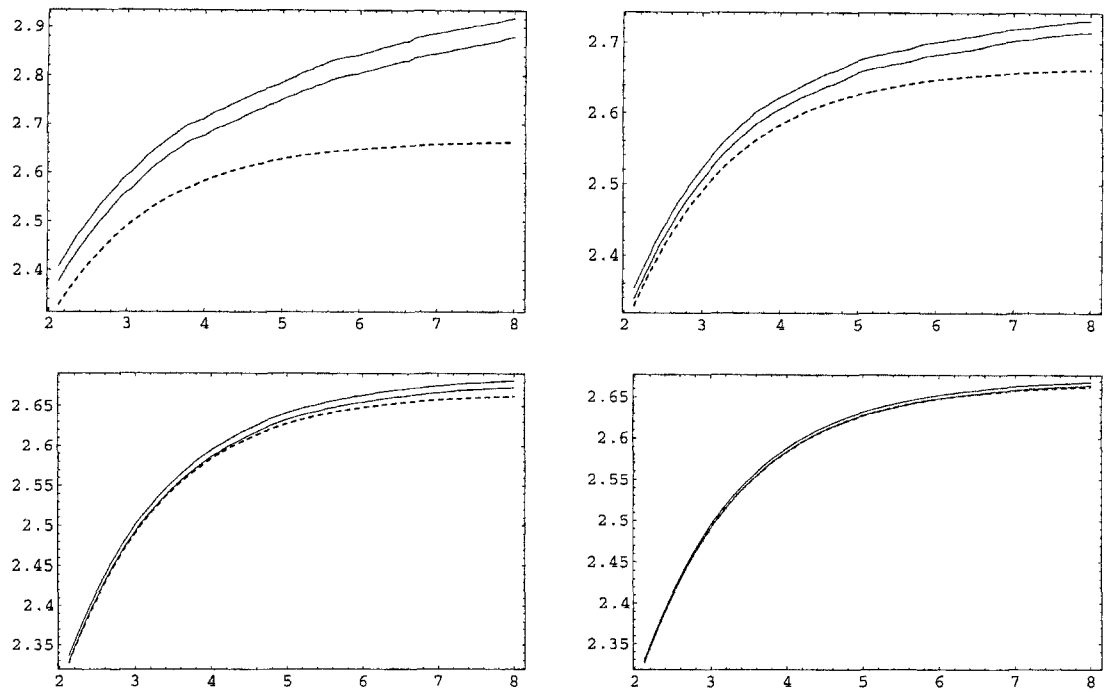

Figure 1. Analytical and numerical solutions for $n = 64$, 256, 1024, and 4096.

Table 1. Numerical convergence, Example 3.

n	$E_{\max}$	CF	$\|V\|_\infty$
64	0.895E − 01	-	0.672E − 02
256	0.235E − 01	3.81	0.516E − 02
1024	0.571E − 02	4.11	0.211E − 02
4096	0.150E − 02	3.81	0.141E − 02
16384	0.305E − 03	4.92	0.355E − 03

$$E_{\max} = \max_{0\le m\le M} \left| \frac{T(t_m) - T_m}{T(t_m)} \right|, \tag{35}$$

where $T(t_m)$ are the exact values of the temperature at time point t_m and T_m is the computed temperature. The third column of Table 1 shows the "convergence factor", i.e., the quotient between the errors in two consecutive lines. This column clearly indicates the linear convergence of the error, i.e., $E_{\max} = O(n^{-1})$. The maximum of the norm of the bulk velocity

$$\|V\|_\infty = \max_{0\le m\le M} |V(t_m)|$$

is presented in the fourth column of Table 1. Thus, this error is well controlled.

EXAMPLE 4. We use the initial condition (33) and the following set of parameters in (1),(4),(7)

$$\beta = \frac{1}{8}, \qquad \gamma = 4, \qquad \alpha = \frac{1}{2}, \qquad C_0 = \frac{1}{4\pi}.$$

Thus, we obtain (cf. (17))

$$T_0 = 1, \qquad T_\infty = \frac{1}{3}$$

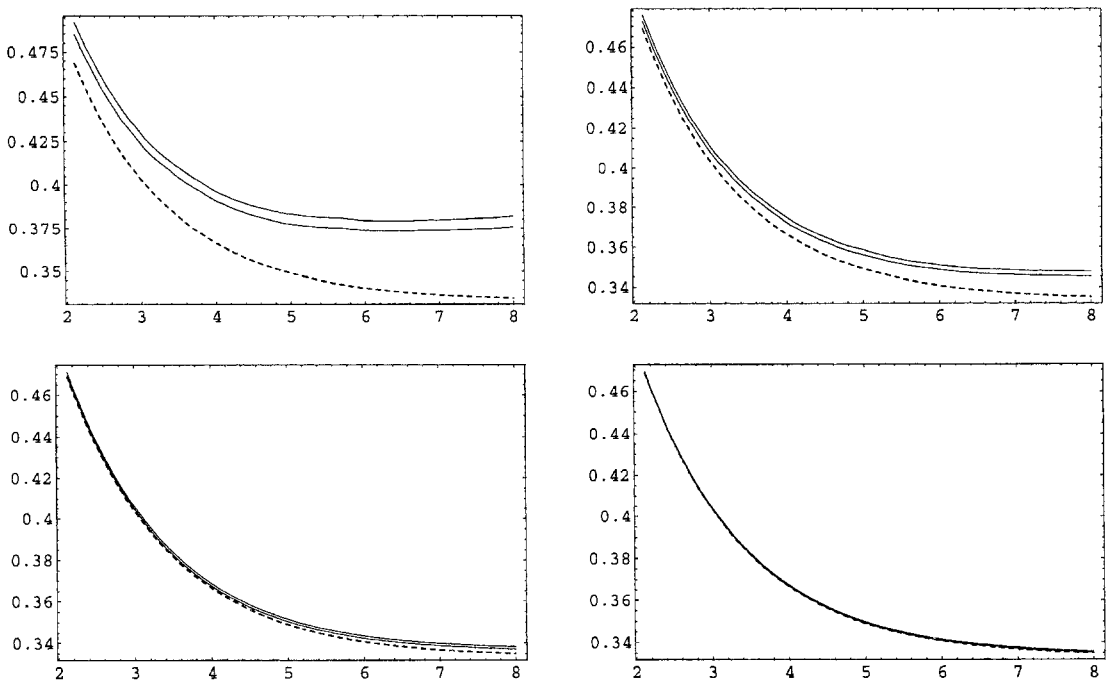

Figure 2. Analytical and numerical solutions for $n = 64$, 256, 1024, and 4096.

Table 2. Numerical convergence, Example 4.

n	$E_{\max}$	CF	$\|V\|_\infty$
64	0.130E − 00	–	0.306E − 02
256	0.336E − 01	3.87	0.188E − 02
1024	0.823E − 02	4.08	0.874E − 02
4096	0.211E − 02	3.90	0.581E − 02
16384	0.455E − 03	4.64	0.148E − 02

and (cf. (16))

$$T(t) = e^{-(3/4)t} + \frac{1}{3}\left(1 - e^{-(3/4)t}\right). \tag{36}$$

Here, the temperature decreases monotonically in time.

The numerical results for Example 4 are displayed in Figure 2, where the curves have the same meaning as in Figure 1.

The relative error of temperature (36) computed corresponding to (35) is presented in Table 2.

EXAMPLE 5. This example illustrates the time relaxation of the temperature for the hard spheres model (6). We use again the initial condition (33) and the following set of parameters in (1),(4),(6)

$$\beta = 0.125, \qquad \gamma = 4, \qquad \alpha = \frac{1}{2}, \qquad C_1 = \frac{1}{4\pi}.$$

Equation (1) is solved on the time interval $[0.0, 2.0]$.

The numerical results for Example 5 are displayed in Figure 3, where the time relaxation of the empirical mean values (cf. (30)) for the temperature using $N = 1000$ independent ensembles are presented. It can be clearly seen that the curves converges for an increasing number of particles to some final curve of the temperature also for the hard spheres model.

REMARK 6. Concerning the convergence ($n \to \infty$) of the stochastic particle methods for the classical, elastic Boltzmann equation, we refer to [34]. The order n^{-1} of the systematic error,

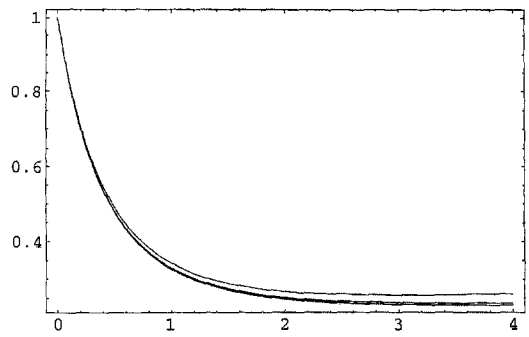

Figure 3. Numerical solutions for $n = 64$, 256, 1024, and 4096 (from above).

which is observed in Tables 1 and 2, seems to be covered by theoretical results concerning Boltzmann like processes with general binary interactions of bounded intensity (cf. [35]). The order of the statistical error is $n^{-1/2}$ so that it is dominated by systematic error only for a certain range of n. This range was made relatively large (out to 4096) in our examples by using $N = 10000$ independent ensembles.

5.3. Asymptotic Tails

In this section, we study the asymptotic behaviour $|v| \to \infty$ of the steady-state distribution function (18) for different values of parameter λ in the VHS-model (8). We assume that the function f_∞ is radially symmetric

$$f_\infty(v) = f_\infty(r), \qquad r = |v|$$

and compute its histogram using uniform discretisation with respect to parameter r, i.e., discretisation of the whole velocity space in a system of concentric shells with increasing radius

$$r_k = kh_r, \qquad k = 1, \dots, K, \quad h_r = \frac{R}{K}. \tag{37}$$

Here $R > 0$ and $K \in \mathbb{N}$ are some additional parameters of the simulation. The histogram of the numerical steady-state solution is then obtained counting the weight of the particles in the corresponding shells

$$f_1 = \frac{1}{n} \# \{v_j : |v_j| < r_1\},$$

$$f_k = \frac{1}{n} \# \{v_j : r_{k-1} \le |v_j| < r_k\}, \qquad k = 2, \dots, K,$$

$$f_{K+1} = \frac{1}{n} \# \{v_j : R \le |v_j|\}.$$

In the following examples, we always use $K = 128$ for the number of shells, $n = 10^7$ for the number of particles and $N = 100$ for the number of independent ensembles.

EXAMPLE 7. We use the Maxwell pseudomolecules model (7), the initial condition (33), and the following set of parameters in (1),(4),(7)

$$\beta = 30, \qquad \gamma = 16, \qquad \alpha = \frac{1}{10}, \qquad C_0 = \frac{1}{4\pi},$$

and $R = 40$ in (37). The time interval is $[0.0, 2.5]$.

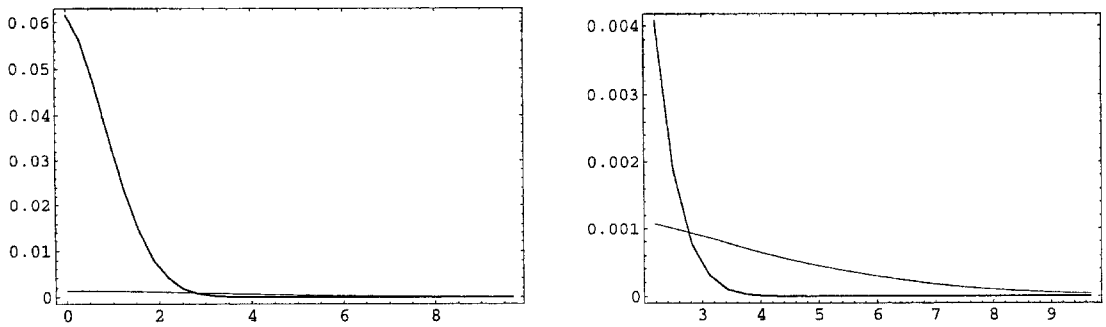

Figure 4. Initial and final histograms, Example 7.

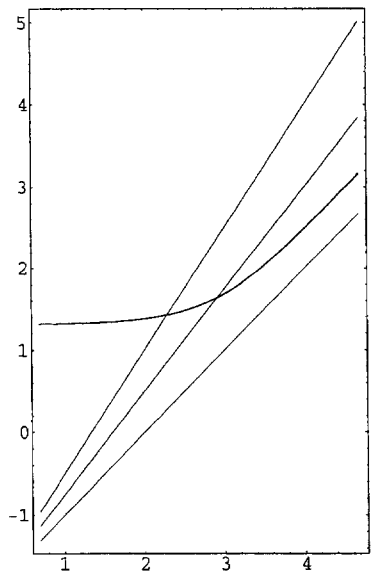

Figure 5. Logarithmic plot of the histogram, Example 7.

The histograms for the initial Maxwell distribution (thick solid line) and for the final numerical distribution (thin solid line) are shown in Figure 4. The left plot shows the histograms for $r \in [0, 10]$ while the right plot shows the "overpopulated tail" of the steady-state distribution function for $r \in [2, 10]$.

In order to obtain the exponent in (19) numerically, we assume

$$f_k = c \exp\left(-a(r_k - r_{k_0})^b\right), \qquad k \geq k_0 \tag{38}$$

and plot the pairs (x_k, y_k)

$$x_k = \ln\left(r_k - r_{k_0}\right), \quad y_k = \ln\left(\ln f_{k_0} - \ln f_k\right), \qquad k = k_0 + 1, \ldots, K.$$

Thus, we expect with $y_k = \ln a + b x_k$ an almost linear plot which slope will show the exponent b in (38). The numerical results are shown in Figure 5, where the thick solid line shows the course of the values y_k computed for $k_0 = 1$ while the thin straight lines $y = x - 2$, $y = 1.25x - 2$, $y = 1.5x - 2$ are drawn for comparison of the slopes. A linear least squares fit of the numerical data on the interval $[4.25, 4.6]$ gives an exponent 0.998. Thus, asymptotics (20) is clearly indicated.

EXAMPLE 8. We consider the hard spheres model (6), the initial condition (33), and the following set of parameters in (1),(4),(6)

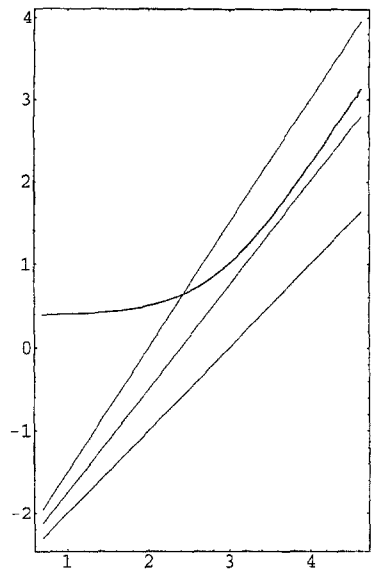

Figure 6. Logarithmic plot of the histogram, Example 8.

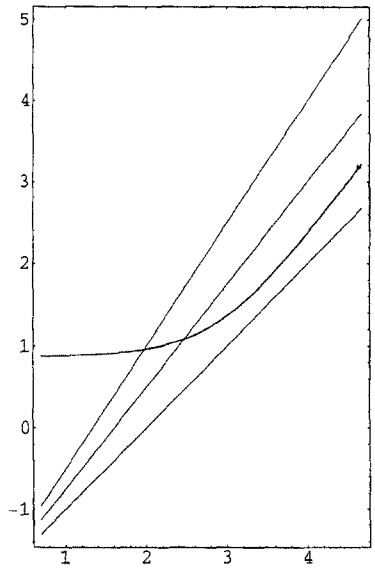

Figure 7. Logarithmic plot of the histogram, Example 9.

$$\beta = 30, \qquad \gamma = 16, \qquad \alpha = \frac{1}{10}, \qquad C_1 = \frac{1}{4\pi},$$

and $R = 16$ in (37). The time interval is $[0.0, 0.25]$.

The numerical results are shown in Figure 6, where the thick solid line shows the course of the values y_k computed for $k_0 = 1$ while the thin straight lines $y = x - 3$, $y = 1.25x - 3$, $y = 1.5x - 3$ are drawn for comparison of the slopes. A linear least squares fit of the numerical data on the interval $[4.25, 4.6]$ gives an exponent 1.474. Thus, the theoretical asymptotics (19) with $b = 1.5$ is clearly indicated.

EXAMPLE 9. We consider now the variable hard spheres model (8) with $\lambda = 0.5$, the initial condition (33), and the following set of parameters in (1),(4),(8)

$$\beta = 30, \qquad \gamma = 16, \qquad \alpha = \frac{1}{10}, \qquad C_0 = \frac{1}{4\pi},$$

and $R = 24$ in (37). The time interval is $[0.0, 0.5]$.

The numerical results are shown in Figure 7, where the thick solid line shows the course of the values y_k computed for $k_0 = 1$ while the thin straight lines $y = x - 2$, $y = 1.25x - 2$, $y = 1.5x - 2$ are drawn for comparison of the slopes. A linear least squares fit of the numerical data on the interval $[4.25, 4.6]$ gives an exponent 1.266. Thus, the theoretical asymptotics (21) with $\lambda = 0.5$ is clearly indicated.

REMARK 10. Though the asymptotic behaviour of the tails can be seen clearly, this type of study is related to modelling of very rare events. The unstable behaviour of the numerical curve for large r in Figures 5–7 is due to difficulties by computing the tails of the distribution function using particles with constant weights. Weighted particles schemes, like SWPM proposed in [36–38] for the classical, elastic Boltzmann equation, might be more efficient for such calculations.

REFERENCES

1. C. Cercignani, Recent developments in the mechanics of granular materials, In *Fisica Matematica e Ingegneria Delle Strutture*, pp. 119–132, Pitagora Editrice, Bologna, (1995).
2. I. Goldhirsch, Rapid granular flows: Kinetics and hydrodynamics, In *Modeling in Applied Sciences, Model. Simul. Sci. Eng. Technol.*, pp. 21–79, Birkhäuser Boston, Boston, MA, (2000).

3. P.B. Umbanhowar, F. Melo and H.L. Swinney, Localized excitations in a vertically vibrated granular layer, *Nature* **382**, 793–796, (1996).
4. J.T. Jenkins and S.B. Savage, A theory for rapid flow of identical, smooth, nearly elastic, spherical particles, *J. Fluid Mech.* **130**, 187–202, (1983).
5. J.T. Jenkins and M.W. Richman, Grad's 13-moment system for a dense gas of inelastic spheres, *Arch. Rational Mech. Anal.* **87** (4), 355–377, (1985).
6. A. Goldshtein and M. Shapiro, Mechanics of collisional motion of granular materials. I. General hydrodynamic equations, *J. Fluid Mech.* **282**, 75–114, (1995).
7. C. Bizon, M.D. Shattuck, J.B Swift and H.L. Swinney, Transport coefficients for granular media from molecular dynamics simulations, *Phys. Rev. E* **64** (3), 4340–4351, (2001).
8. S.J. Moon, M.D. Shattuck and J.B. Swift, Velocity distributions and correlations in homogeneously heated granular media, *Phys. Rev. E* **64**, 031303-1–031303-10, (2001).
9. N.V. Brilliantov and T. Poeschel, *Granular Gases with Impact-velocity Dependent Restitution Coefficient, Granular Gases, Lecture Notes in Physics, Volume 564*, (Edited by T. Poeschel and S. Luding) pp. 100–124, Springer, Berlin, (2000).
10. D.R.M. Williams and F.C. MacKintosh, Driven granular media in one dimension: Correlations and equation of state, *Phys. Rev. E* **54**, 9–12, (1996).
11. T.P.C. van Noije and M.H. Ernst, Velocity distributions in homogeneously cooling and heated granular fluids, *Gran. Matt.* **1**, 57, (1998).
12. J.A. Carrillo, C. Cercignani and I.M. Gamba, Steady states of a Boltzmann equation for driven granular media, *Phys. Rev. E (3)* **62** (6, Part A), 7700–7707, (2000).
13. A.V. Bobylev, J.A. Carrillo and I.M. Gamba, On some properties of kinetic and hydrodynamic equations for inelastic interactions, *J. Statist. Phys.* **98** (3-4), 743–773, (2000).
14. P.L. Krapivsky and E. Ben-Naim, Multiscaling in infinite dimensional collision processes, *Phys. Rev. E* **61** (R5), (2000).
15. P.L. Krapivsky and E. Ben-Naim, Nontrivial velocity distributions in inelastic gases, *J. Phys. A* **35** (L147), (2002).
16. M.H. Ernst and R. Brito, Scaling solutions of inelastic Boltzmann equations with over-populated high energy tails, *J. Statist. Phys.* **109** (3-4), 407–432, (2002).
17. A. Baldassarri, U. Marini Bettolo Marconi and A. Puglisi, Kinetic Models of Inelastic Gases, *Mathematical Models and Methods in Applied Science* **12** (7), 965–983, (2002).
18. A.V. Bobylev and C. Cercignani, Moment equations for a granular material in a thermal bath, *J. Statist. Phys.* **106** (3-4), 547–567, (2002).
19. C. Cercignani, R. Illner and C. Stoica, On diffusive equilibria in generalized kinetic theory, *J. Statist. Phys.* **105** (1-2), 337–352, (2001).
20. I.M. Gamba, V. Panferov and C. Villani, On the Boltzmann equation for diffusively excited granular media, *Comm. Math. Phys.* **246** (3), 503–541, (2004).
21. C. Cercignani, R. Illner and M. Pulvirenti, *The Mathematical Theory of Dilute Gases*, Springer, New York, (1994).
22. G.A. Bird, Monte Carlo simulation in an engineering context, *Progr. Astro. Aero* **74**, 239–255, (1981).
23. A.V. Bobylev and C. Cercignani, Moment equations for a granular material in a thermal bath, *J. Statist. Phys.* **106** (3-4), 547–567, (2002).
24. A.V. Bobylev, M. Groppi and G. Spiga, Approximate solutions to the problem of stationary shear flow of smooth granular materials, *Eur. J. Mech. B Fluids* **21** (1), 91–103, (2002).
25. D. Benedetto, E. Caglioti, J.A. Carrillo and M. Pulvirenti, A non-Maxwellian steady distribution for one-dimensional granular media, *J. Statist. Phys.* **91** (5-6), 979–990, (1998).
26. A.V. Bobylev, I.M. Gamba and V. Panferov, Moment inequalities and high-energy tails for Boltzmann equations with inelastic interactions, *J. Statist. Phys.* **116** (5-6), 1651–1682, (2004).
27. W. Losert, D.G.W. Cooper, J. Delour, A. Kudrolli and J.P. Gollub, Velocity statistics in excited granular media, *Chaos* **9** (3), 682–690, (1999).
28. A. Kudrolli and J. Henry, Non-Gaussian velocity distributions in excited granular matter in the absence of clustering, *Phys. Rev. E* **62** (R1489), (2000).
29. F. Rouyer and N. Menon, Velocity fluctuations in a homogeneous 2d granular gas in steady state, *Phys. Rev. Lett.* **85**, 3676, (2000).
30. G.A. Bird, *Molecular Gas Dynamics and the Direct Simulation of Gas Flows*, Clarendon Press, Oxford, (1994).
31. J.J. Brey, M.J. Ruiz-Montero and D. Cubero, Homogeneous cooling state of a low-density granular flow, *Phys. Rev. E* **54** (4), 3664–3671, (1996).
32. J.M. Montanero and A. Santos, Computer simulation of uniformly heated granular fluids, *Granular Matter* **2**, 53–64, (2000).
33. A. Barrat, T. Biben, Z. Rácz, E. Trizac and F. van Wijland, On the velocity distributions of the one-dimensional inelastic gas, *J. Phys. A: Math. Gen.* **35**, 463–480, (2002).
34. W. Wagner, A convergence proof for Bird's direct simulation Monte Carlo method for the Boltzmann equation, *J. Statist. Phys.* **66** (3/4), 1011–1044, (1992).
35. C. Graham and S. Méléard, Stochastic particle approximations for generalized Boltzmann models and convergence estimates, *Ann. Probab.* **25** (1), 115–132, (1997).

36. S. Rjasanow and W. Wagner, A stochastic weighted particle method for the Boltzmann equation, *J. Comp. Phys.* **124**, 243–253, (1996).
37. S. Rjasanow and W. Wagner, Simulation of rare events by the stochastic weighted particle method for the Boltzmann equation, *Mathl. Comput. Modelling* **33** (8/9), 907–926, (2001).
38. S. Rjasanow and W. Wagner, *Stochastic Numerics for the Boltzmann Equation*, Springer, Berlin, (2005).